

## LETTER

# Continuous-Phase, Unmodulated Parallel-Combinatory High-Compaction Multicarrier Modulation\*

Ryuji HAYASHI<sup>†a)</sup>, Student Member and Masanori HAMAMURA<sup>†</sup>, Member

**SUMMARY** A new type of modulation called continuous-phase parallel-combinatory high-compaction multicarrier modulation (CPPC/HC-MCM) is proposed. CPPC/HC-MCM employs the technique of continuous-phase modulation (CPM) and avoids the formation of amplitude gaps between two successive signals to enhance the spectral efficiency of conventional PC/HC-MCM. Results of simulations show that CPPC/HC-MCM is spectrally efficient and achieves a smaller bit error rate than conventional (unmodulated) PC/HC-MCM at a common spectral efficiency even if the peak-to-average power ratio is considered.

**key words:** PC signaling, HC-MCM, continuous-phase modulation, spectral efficiency

## 1. Introduction

Spectral efficiency is an important parameter in designing wireless communication systems. Orthogonal frequency-division multiplexing (OFDM) achieves high spectral efficiency and has robustness against the intersymbol interference (ISI) caused by channel multipath. One major drawback of OFDM is the high peak-to-average power ratio (PAR) of the transmitting signals. To reduce the PAR and improve the spectral efficiency and bit error rate (BER), parallel-combinatory OFDM (PC-OFDM) [1] and parallel-combinatory high-compaction multicarrier modulation (PC/HC-MCM) [2] using the technique of PC signaling [3] were proposed. Since PC/HC-MCM transmits a truncated version of the PC-OFDM signal, amplitude discontinuities between two successive signal waveforms appear, resulting in unnecessary bandwidth spread. Therefore, it is expected that the unnecessary bandwidth spread can be reduced in PC/HC-MCM by avoiding the formation of amplitude gaps.

In this paper, we discuss continuous-phase PC/HC-MCM (CPPC/HC-MCM) using the technique of continuous-phase modulation (CPM) [4], [5] and demonstrate that CPPC/HC-MCM improves the spectral efficiency of PC/HC-MCM and results in an improvement of the BER performance at a fixed spectral efficiency even if the PAR is

considered.

## 2. PC-OFDM and PC/HC-MCM

PC-OFDM is a type of OFDM that conveys message data by PC signaling together with ordinary  $M$ -ary amplitude and phase shift keying ( $M$ -APSK).

Let  $M_c$  be the total number of all preassigned carriers, and let  $M_p$  be the number of carriers selected for PC signaling. In this case, the number of message data bits per PC-OFDM signal,  $m_{total}$  [bits], is represented as

$$m_{total} = m_{apks} + m_{pc}, \quad (1)$$

where  $m_{apks}$  [bits] is the number of message data bits mapped into  $M$ -APSK constellations of  $M_p$  carriers, given by

$$m_{apks} = M_p \log_2 M, \quad (2)$$

and  $m_{pc}$  [bits] is the number of message data bits encoded into one of the prescribed sets of  $M_p$  carriers, that is,

$$m_{pc} = \left\lfloor \log_2 \binom{M_c}{M_p} \right\rfloor. \quad (3)$$

$\lfloor \cdot \rfloor$  is an operator that denotes the largest integer that is less than or equal to the operand.

The PC-OFDM signals are modeled using the lowpass equivalent notation such that

$$y(t) = \sum_{n=0}^{\infty} s^{(n)}(t - nT_s) \quad (4)$$

$$s^{(n)}(t) = \sum_{l=1}^{M_c} x_l^{(n)} e^{j2\pi(l-1)\Delta f t}, \quad 0 \leq t < T_s, \quad (5)$$

where  $x_l^{(n)}$  ( $l = 1, 2, \dots, M_c$ ) is the complex symbol for the  $l$ th carrier, which takes an  $M$ -APSK constellation including zero amplitude, in  $nT_s \leq t < (n+1)T_s$ ,  $\Delta f$  [Hz] is the frequency spacing, and  $T_s$  [s] is the symbol duration and is chosen to be  $T_s = 1/\Delta f$  in PC-OFDM.

Here,  $m_{pc}$  message data bits can be transmitted by selecting appropriate  $M_p$  carriers without  $M$ -APSK in PC-OFDM. In this case,  $x_l^{(n)}$  is chosen to be  $x_l^{(n)} = 1$  if the  $l$ th carrier is selected and  $x_l^{(n)} = 0$  otherwise. Therefore,  $x_l^{(n)} = \{0, 1\}$ , and  $m_{total}$  is reduced to  $m_{total} = m_{pc}$ .

PC/HC-MCM is categorized into two systems: modulated and unmodulated. Modulated PC/HC-MCM transmits

Manuscript received July 13, 2010.

Manuscript revised November 16, 2010.

<sup>†</sup>The authors are with the Graduate School of Engineering, Kochi University of Technology, Kami-shi, 782-8502 Japan.

\*This work is based on "Performance of Continuous-Phase, Unmodulated Parallel-Combinatory High-Compaction Multicarrier Modulation," by R. Hayashi and M. Hamamura, which appeared in Proc. IEEE International Wireless Communications and Mobile Computing Conference (IWCMC 2008), Crete, Greece, Aug. 2008, ©2008 IEEE.

a) E-mail: r.hayashi@m.ieice.org

DOI: 10.1587/transcom.E94.B.802

a truncated PC-OFDM signal, and unmodulated PC/HC-MCM transmits a truncated PC-OFDM signal without  $M$ -APSK modulation. Thus, the PC/HC-MCM signals are also modeled using (4) and (5) with  $T_s < 1/\Delta f$ .

In this paper, we consider the use of unmodulated PC/HC-MCM to improve the spectral efficiency, resulting in an improvement in BER. Hereafter, we simply refer to unmodulated PC/HC-MCM as PC/HC-MCM.

### 3. CPPC/HC-MCM

#### 3.1 CPPC/HC-MCM Signal and Its Transmitter

Let  $\mathcal{A} = \{k \in \mathbb{N} | 1 \leq k \leq M_c\}$  be the set of indices of all pre-assigned carriers, and let  $\mathcal{B}^{(n)} = \{b_1^{(n)}, b_2^{(n)}, \dots, b_{M_p}^{(n)}\} \subset \mathcal{A}$  ( $|\mathcal{B}^{(n)}| = M_p$ ) be a subset of  $\mathcal{A}$  consisting of the complete set of indices of carriers used for PC signaling in  $nT_s \leq t < (n+1)T_s$ .  $\mathcal{B}^{(n)}$  is one of the possible subsets, that is,  $\mathcal{B}^{(n)} \in \mathcal{C} = \{\mathcal{B}_1, \mathcal{B}_2, \dots, \mathcal{B}_{2^{m_{pc}}}\}$ , and without loss of generality, we assume that  $b_1^{(n)} < b_2^{(n)} < \dots < b_{M_p}^{(n)}$ . Using this notation, the PC/HC-MCM signal given by (5) can be rewritten as

$$s^{(n)}(t) = \sum_{l \in \mathcal{B}^{(n)}} e^{j2\pi(l-1)\Delta f t}, \quad 0 \leq t < T_s. \quad (6)$$

To avoid amplitude gaps between two successive PC/HC-MCM signals, we employ phase modulation in CPPC/HC-MCM. The CPPC/HC-MCM signal is given by

$$s^{(n)}(t) = \sum_{l \in \mathcal{B}^{(n)}} \zeta_l^{(n)} e^{j2\pi(l-1)\Delta f t}, \quad 0 \leq t < T_s, \quad (7)$$

where  $\zeta_l^{(n)}$  ( $l \in \mathcal{B}^{(n)}$ ) are the complex-valued phase rotators recursively defined as

$$\begin{aligned} \zeta_{b_1^{(n+1)}}^{(n+1)} &= \zeta_{b_1^{(n)}}^{(n)} e^{j2\pi(b_1^{(n)}-1)\Delta f T_s} \\ \zeta_{b_2^{(n+1)}}^{(n+1)} &= \zeta_{b_2^{(n)}}^{(n)} e^{j2\pi(b_2^{(n)}-1)\Delta f T_s} \\ &\vdots \\ \zeta_{b_{M_p}^{(n+1)}}^{(n+1)} &= \zeta_{b_{M_p}^{(n)}}^{(n)} e^{j2\pi(b_{M_p}^{(n)}-1)\Delta f T_s}. \end{aligned} \quad (8)$$

We assume that  $\zeta_l^{(0)} = 1$  ( $l \in \mathcal{B}^{(0)}$ ) for  $n = 0$ , and undefined phase rotators  $\zeta_l^{(n)}$  ( $l \notin \mathcal{B}^{(n)}$ ) can be chosen to be zero. Note that the PC/HC-MCM signals given by (6) can be represented by  $\zeta_l^{(n)} = 1$  ( $l \in \mathcal{B}^{(n)}$ ) for all  $n$ ) as a special case of the CPPC/HC-MCM signals. Also note that the CPPC/HC-MCM signals given by (7) become the well-known full-response CPM signals if  $M_p = 1$ .

Figure 1 shows the transmitter used for CPPC/HC-MCM. The time index  $n$  is omitted in Fig. 1. At the transmitter,  $m_{pc}$  data bits are serial-to-parallel (S/P) converted and mapped into the corresponding combination of carriers by a PC mapper. After the PC mapping, the phase rotators rotate the phase of carriers in accordance with the rule given by (8). After the phase rotation,  $M_0$  zeros are added on to the sequence of complex symbols  $x_l^{(n)} \zeta_l^{(n)}$  ( $l = 1, 2, \dots, M_c$ ) at

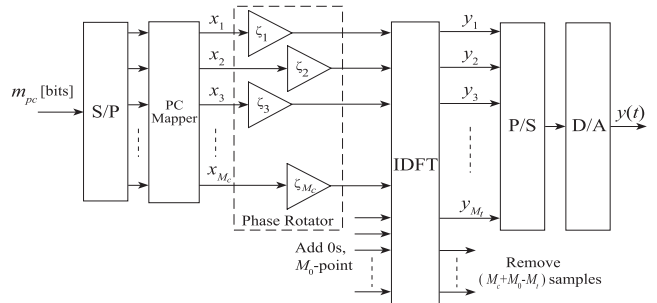


Fig. 1 IDFT-based transmitter of CPPC/HC-MCM.

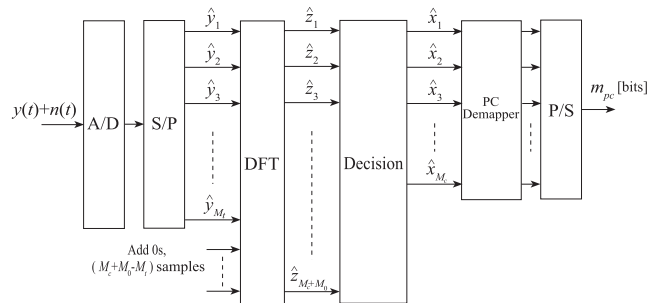


Fig. 2 DFT-based receiver of CPPC/HC-MCM.

the input of the inverse discrete Fourier transform (IDFT). After the IDFT, we obtain  $M_c + M_0$  samples and remove  $(M_c + M_0 - M_t)$  samples. Therefore, only  $M_t$  samples are used for parallel-to-serial (P/S) conversion and digital-to-analog (D/A) conversion to produce the transmitting signal  $y(t)$ . The operation for removing  $(M_c + M_0 - M_t)$  samples corresponds to the truncation of the waveform using the rectangular window function in the time domain.

#### 3.2 Receiver

Figure 2 shows the receiver used for CPPC/HC-MCM. The signal  $y(t)$  is received in the presence of additive white Gaussian noise (AWGN)  $n(t)$ .  $M_t$  discrete-time samples  $\hat{y}_m$  ( $m = 1, 2, \dots, M_t$ ) are obtained using the analog-to-digital (A/D) converter and are S/P converted. The samples  $\hat{y}_m$  are converted to the frequency domain samples  $\hat{z}_k$  ( $k = 1, 2, \dots, M_c + M_0$ ) by the discrete Fourier transform (DFT) with  $(M_c + M_0 - M_t)$ -point zero padding.

At the decision stage of the receiver, it is possible to utilize one of the many types of detection scheme developed for CPM. In this paper, we adopt maximum likelihood (ML) detection to simplify the discussion and to show an achievable limit for BER performance.

Let  $\mathcal{P}^{(n)} = \{\zeta_{b_1^{(n)}}^{(n)}, \zeta_{b_2^{(n)}}^{(n)}, \dots, \zeta_{b_{M_p}^{(n)}}^{(n)}\} \in \mathcal{D} = \{\mathcal{P}_1, \mathcal{P}_2, \dots, \mathcal{P}_{|\mathcal{D}|}\}$  be the set of values of  $M_p$  nonzero phase rotators. Then, ML detection determines which PC signal, characterized by the set  $\mathcal{B}^{(n)}$  of indices of carriers, was transmitted. In this problem, from all possible sets of  $\mathcal{B}$ , we find the set  $\hat{\mathcal{B}}$  that satisfies

$$\hat{\mathcal{B}} = \arg \min_{\mathcal{B} \in \mathcal{C}, \mathcal{P} \in \mathcal{D}} \left( J(\mathcal{B}, \mathcal{P}) = \sum_{k=1}^{M_c+M_0} |\hat{z}_k - z_{\mathcal{B}, \mathcal{P}, k}|^2 \right), \quad (9)$$

where  $z_{\mathcal{B}, \mathcal{P}, k}$  ( $k = 1, 2, \dots, M_c + M_0$ ) are the replica samples, that is, the noiseless version of frequency domain samples  $\hat{z}_k$  for  $\mathcal{B} \in \mathcal{C}$  and  $\mathcal{P} \in \mathcal{D}$ .

To reduce the complexity required for ML detection, it is reasonable to choose the value of  $1/\Delta f T_s$  to be an integer in CPPC/HC-MCM. In this case, since  $|\mathcal{D}| = (1/\Delta f T_s)^{M_p}$ , the complexity of ML detection for CPPC/HC-MCM increases by a factor of  $(1/\Delta f T_s)^{M_p}$  in comparison with that for PC/HC-MCM.

#### 4. Performance of CPPC/HC-MCM

We compare the performance characteristics of CPPC/HC-MCM and PC/HC-MCM in terms of the required bandwidth, spectral efficiency, BER, and PAR by performing simulations. We assume the Gray code mapping/demapping as the PC mapper/demapper. One example of the PC mapping/demapping for  $\binom{M_c}{M_p} = \binom{8}{2}$  is shown in Table 1.

There are several definitions for the bandwidth of signals [6]. The popular measures are the half-power bandwidth, null-to-null bandwidth, root-mean-square (RMS) bandwidth, and fractional power bandwidth. In this paper, we discuss the fractional power bandwidth of the CPPC/HC-MCM signals using a  $2^{15}$ -point DFT, for which we adopt a 99% power containment, as commonly considered in regulations (e.g., [6]). The results of our simulations are shown in Fig. 3.

It was observed that CPPC/HC-MCM greatly reduces the required bandwidth of PC/HC-MCM. The bandwidths of the PC/HC-MCM signals are identical for all values of  $M_p$ , but the bandwidth of CPPC/HC-MCM signals depends on  $M_p$ . The larger the value of  $M_p$ , the narrower the 99% bandwidth of CPPC/HC-MCM. For example, CPPC/HC-MCM occupies 99% bandwidths of  $22.5/T_s$  at  $\Delta f = 0.5/T_s$  for  $M_p = 2$ , and  $13.5/T_s$  for  $M_p = 7$ . The 99% bandwidth of CPPC/HC-MCM for  $\binom{M_c}{M_p} = \binom{8}{7}$  is half the bandwidth of PC/HC-MCM. Power density spectra of the low-pass equivalent CPPC/HC-MCM signals are shown in Fig. 4 for  $M_p = 2, 4$ , and 7 at  $\Delta f = 0.5/T_s$ . It is verified from Fig. 4 that the tails of the spectra smoothly decay.

Next, we discuss the spectral efficiency  $\eta$  of CPPC/HC-

MCM, which is defined as

$$\eta = \frac{m_{pc} \cdot 1/T_s}{W_{99\%}} = \frac{\lfloor \log_2 \binom{M_c}{M_p} \rfloor}{W_{99\%} T_s}, \quad (10)$$

where  $W_{99\%}$  denotes the 99% bandwidth.

Figure 5 shows the spectral efficiencies of PC/HC-MCM and CPPC/HC-MCM as functions of the frequency spacing  $\Delta f$ . CPPC/HC-MCM achieves a higher spectral efficiency than PC/HC-MCM for all  $M_p$ . Note that the spectral efficiency of PC/HC-MCM for  $\binom{M_c}{M_p}$  is identical to that of PC/HC-MCM for  $\binom{M_c}{M_c - M_p}$ ; however, the spectral efficiencies of CPPC/HC-MCM for  $\binom{M_c}{M_p}$  and  $\binom{M_c}{M_c - M_p}$  are different. For example,  $\eta = 0.18$  at  $\Delta f = 0.5/T_s$  for  $\binom{M_c}{M_p} = \binom{8}{2}$ , but  $\eta = 0.25$  for  $\binom{M_c}{M_p} = \binom{8}{6}$ .

Figure 6 shows the BER vs. spectral efficiency  $\eta$  characteristics. It is seen from Fig. 6 that all the plots for PC/HC-MCM are shifted to the right using the proposed phase modulation given by (8). This comes from the fact that, because

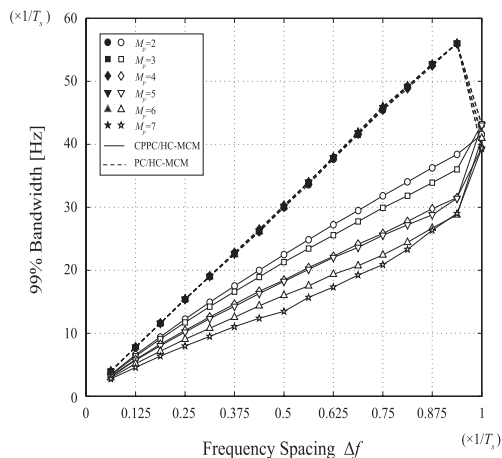


Fig. 3 Bandwidth vs. frequency spacing  $\Delta f$  for CPPC/HC-MCM and PC/HC-MCM ( $M_c = 8$ ).

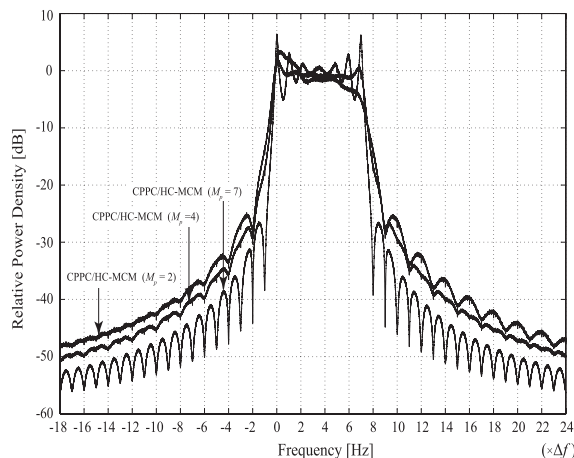


Fig. 4 Power density spectra of CPPC/HC-MCM signals ( $M_c = 8$ ,  $\Delta f T_s = 0.5$ ).

Table 1 An example of PC mapping/demapping using the Gray code for  $\binom{M_c}{M_p} = \binom{8}{2}$ .

Message data	$\mathcal{B}^{(n)}$	Frequencies	$x_1$ $x_2$ $\dots$ $x_8$
100	{1, 2}	$\{f_1, f_2\}$	1 1 0 0 0 0 0 0
101	{1, 3}	$\{f_1, f_3\}$	1 0 1 0 0 0 0 0
111	{1, 4}	$\{f_1, f_4\}$	1 0 0 1 0 0 0 0
110	{1, 5}	$\{f_1, f_5\}$	1 0 0 0 1 0 0 0
010	{1, 6}	$\{f_1, f_6\}$	1 0 0 0 0 1 0 0
011	{1, 7}	$\{f_1, f_7\}$	1 0 0 0 0 0 1 0
001	{1, 8}	$\{f_1, f_8\}$	1 0 0 0 0 0 0 1
000	{2, 3}	$\{f_2, f_3\}$	0 1 1 0 0 0 0 0

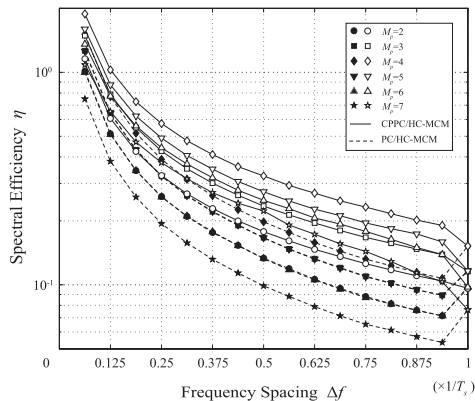
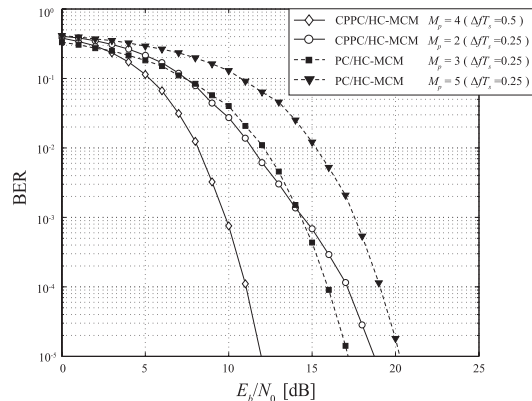


Fig. 5 Spectral efficiency vs. frequency spacing  $\Delta f$  for CPPC/HC-MCM and PC/HC-MCM ( $M_c = 8$ ).



(a) BER performance

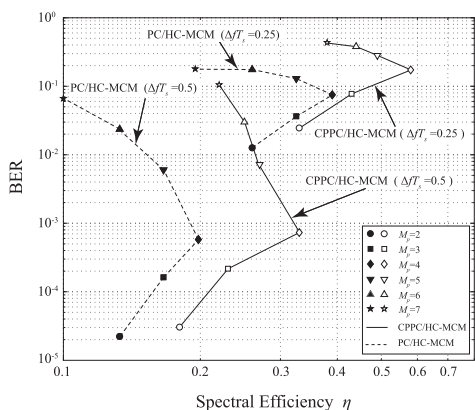
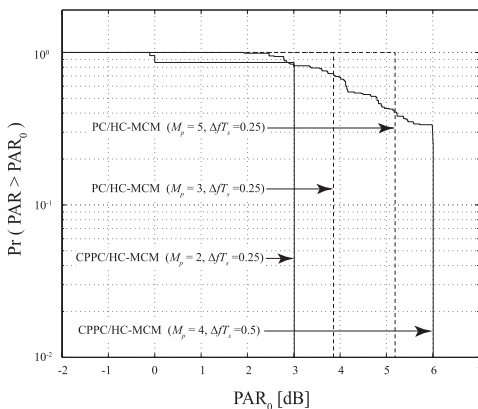


Fig. 6 BER vs. spectral efficiency ( $M_c = 8$ ,  $E_b/N_0 = 10$  dB).



(b) PAR

of its narrower bandwidth property, CPPC/HC-MCM can choose a larger  $\Delta f T_s$  than PC/HC-MCM at the same spectral efficiency so that the receiver can correctly recover the message data.

Finally, we show the BER vs.  $E_b/N_0$  characteristics and complementary cumulative distribution functions (CCDFs)  $\Pr(\text{PAR} > \text{PAR}_0)$  at a common spectral efficiency of  $\eta \approx 0.33$  in Figs. 7(a) and (b), respectively. PAR was defined as

$$\text{PAR} = \max_{0 \leq t < T_s} |s^{(n)}(t)|^2 / \overline{|y(t)|^2}. \quad (11)$$

Figure 7(a) shows that CPPC/HC-MCM achieves a BER of  $10^{-4}$  at  $E_b/N_0 \approx 17.1$  dB for  $M_p = 2$  and at  $E_b/N_0 \approx 11.0$  dB for  $M_p = 4$ , whereas PC/HC-MCM requires  $E_b/N_0 \approx 15.9$  dB for  $M_p = 3$  and  $E_b/N_0 \approx 19.1$  dB for  $M_p = 5$  to achieve  $\eta \approx 0.33$  with the 99% bandwidth criterion. On the other hand, Fig. 7(b) shows that, in CPPC/HC-MCM, PAR reaches 3.0 dB for  $M_p = 2$  and 6.0 dB for  $M_p = 4$ , whereas, in PC/HC-MCM, it reaches 3.8 dB for  $M_p = 3$  and 5.2 dB for  $M_p = 5$ . It is verified that the overall BER performance, including the loss due to PAR, of CPPC/HC-MCM for  $M_p = 4$  is superior to that of PC/HC-MCM for  $M_p = 3$  and 5, because compared with PC/HC-MCM, CPPC/HC-MCM achieves an improvement in BER of more than 4.9 dB which more than offsets its 2.2 dB drop in PAR.

Fig. 7 BER and PAR characteristics of CPPC/HC-MCM and PC/HC-MCM ( $M_c = 8$ ,  $\eta \approx 0.33$ ).

### 5. Conclusion

In this paper, we introduced CPPC/HC-MCM and evaluated its spectral efficiency, BER and PAR. The 99% bandwidth criterion was considered. Simulations showed that CPPC/HC-MCM signals are spectrally efficient and exhibit better BER performance at the same spectral efficiency.

### References

- [1] P.K. Frenger, N. Arne, and B. Svensson, "Parallel combinatory OFDM signaling," IEEE Trans. Commun., vol.47, no.4, pp.558–565, April 1999.
- [2] Y. Hou and M. Hamamura, "A novel modulation with parallel combinatory and high compaction multi-carrier modulation," IEICE Trans. Fundamentals, vol.E90-A, no.11, pp.2556–2567, Nov. 2007.
- [3] S. Sasaki, H. Kikuchi, J. Zhu, and G. Marubayashi, "Multiple access performance of parallel combinatory spread spectrum communication systems in nonfading and Rayleigh fading channels," IEICE Trans. Commun., vol.E78-B, no.8, pp.1152–1161, Aug. 1991.
- [4] T. Aulin and C.-E.W. Sundberg, "Continuous phase modulation-Part I: Full response signaling," IEEE Trans. Commun., vol.COM-29, no.3, pp.196–209, March 1981.
- [5] G. Proakis, Digital Communications, 4th ed., pp.185–192, McGraw-Hill, 2001.
- [6] B. Sklar, Digital Communications, 2nd ed., pp.45–49, Prentice Hall, 2001.